Available online at www.sciencedirect.com
ScienceDirect
Carbohydrate Research 342 (2007) 1918–1928
Carbohydrate RESEARCH

The conformation of the *C*-glycosyl analogue of *N*-acetyl-lactosamine in the free state and bound to a toxic plant agglutinin and human adhesion/growth-regulatory galectin-1

Víctor García-Aparicio,[d] Matthieu Sollogoub,[a,b] Yves Blériot,[a,b] Virginie Colliou,[a,b] Sabine André,[c] Juan L. Asensio,[d] F. Javier Cañada,[d] Hans-Joachim Gabius,[c] Pierre Sinaÿ[a,b] and Jesús Jiménez-Barbero[d,*]

[a]*Ecole Normale Supérieure, Département de Chimie, UMR CNRS 8642, 24, rue Lhomond, 75231 Paris Cedex 05, France*
[b]*Université Pierre et Marie Curie-Paris 6, Institut de Chimie Moléculaire (FR 2769), 75005 Paris, France*
[c]*Institut für Physiologische Chemie, Tierärztliche Fakultät, Ludwig-Maximilians-Universität, Veterinärstr. 13, 80539 München, Germany*
[d]*Departamento de Estructura y Función de Proteínas, Centro de Investigaciones Biológicas, CSIC, Ramiro de Maeztu 9, 28040 Madrid, Spain*

Received 16 January 2007; received in revised form 19 February 2007; accepted 21 February 2007
Available online 4 March 2007

Abstract—The conformational behavior of the C-glycoside analogue of *N*-acetyl-lactosamine, β-*C*-Gal-(1→4)-β-GlcNAc-OMe, **1**, has been studied using a combination of molecular mechanics calculations and NMR spectroscopy (*J* and NOE data). It is shown that the C-disaccharide populates three distinctive conformational families in solution, the major one being the *anti*-ψ conformation. Of note, this conformation is only marginally populated for the O-disaccharide. Due to its conspicuous role in the regulation of adhesion, growth and tissue invasion of tumors and its avid binding to *N*-acetyl-lactosamine human, galectin-1 was tested as a receptor. This endogenous lectin recognizes a local minimum of **1**, the *syn*-ΦΨ conformer, and thus a conformational selection process is correlated with the molecular recognition event.

Keywords: C-Glycosides; Conformational analysis; Glycomimetics; Molecular recognition; NMR

1. Introduction

The search for new glycomimetics has led to a group of compounds, denoted as C-glycosides, in which the anomeric oxygen has been replaced by a methylene group.[1] The determination of the conformational features of C-glycosides and its comparison with that of respective O-glycosides is of primary importance to define the potential of C-analogues as molecular probes. A detailed conformational analysis of a number of C-disaccharides has revealed that the previously postulated conformational similarity between O- and C-glycosides[2] is yet not a general phenomenon.[3] Indeed, C-mannobiose presents significant differences relative to its parent O-glycoside.[4] These findings have encouraged us to extend the comparison between C- and O-glycosides to other pairs. Along these lines, we now report the conformational analysis of the C-disaccharide β-*C*-Gal-(1→4)-β-GlcNAc-OMe[5] (**1**) in water using NMR spectroscopy assisted by molecular mechanics calculations, and a comparison with the parent O-disaccharide (**2**). The β-(1→4)-linkage has been previously studied for the O/C-lactose pair in the free[6] and bound states.[7] However, *N*-acetyl-lactosamine is the natural form of the ligands for lectins that recognize branch-end epitopes of glycan chains, giving this analysis conspicuous physiological relevance.[8] To underscore the potential medical

* Corresponding author. E-mail: jjbarbero@cib.csic.es

0008-6215/$ - see front matter © 2007 Elsevier Ltd. All rights reserved.
doi:10.1016/j.carres.2007.02.034

relevance, some features of the molecular recognition process of **1** by two lectins have been addressed, that is, toxin/agglutinin from mistletoe and human galectin-1, which is known to influence adhesion, growth and tumor invasion.[9]

2. Results and discussion

The key NMR data in D_2O of compound **1** are listed in Table 1 and in Supplementary data. The 1D spectrum yielded the best *J* values for **1** and indicated that the two six-membered rings adopt the usual $^4C_1$ chair. Although this usually is the case, in some cases alternative chair conformations have been described for other *C*-glycosyl compounds.[10]

bridge was exclusively based on experimental *J* and NOE data. This analysis allowed us to identify the presence of a major Φ rotamer (large $J_{H1Gal/HproR}$ value, 10.3 Hz) and the existence of an equilibrium around Ψ (intermediate $J_{H4GlcNAc/HproR}$ and $J_{H4GlcNAc/HproS}$ *J* values, 3.3 and 5.2 Hz, respectively). To properly understand its ligand properties, further characterization of the possible conformers in the conformational equilibrium and of their relative populations is necessary. Therefore, as a next step, molecular mechanics and dynamics calculations were performed.[11]

The potential energy surfaces in the *Φ*/*Ψ*-angle space for four independent starting geometries of **1** (varying the C5–C6 *ω* torsion[12] for the Gal (gt/tg) and GlcNAc (gg/gt) moieties) were calculated with the MM3* force field[13] as integrated in MACROMODEL,[14] and compared

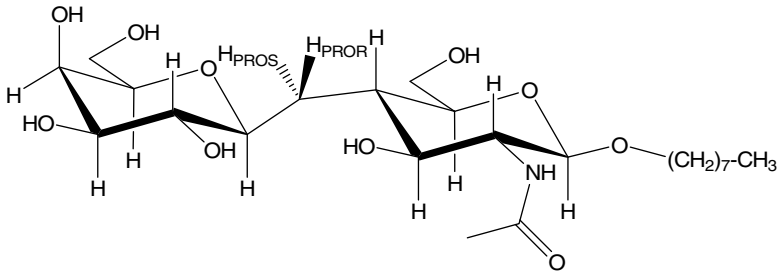

The coupling constants also afforded information on the conformational distribution around the torsional degrees of freedom of the disaccharide (*Φ* and *Ψ* angles). From the inspection of the *J* values (Table 1) it can be deduced that those for **1** are rather similar to those reported for the *C*-glycosyl analogue of lactose, which has been studied previously.[6,7]

The unambiguous assignment of signals from the prochiral methylene protons attached at the glycosidic

to those of the parental O-glycoside (see Table 2). Four and three minima are predicted for the C- and O- compounds, and with completely different relative population densities.

A combination of four conformational families was predicted to co-exist from these MM3* simulations. Therefore, three additional families, apart of the major one described for *N*-acetyl-lactosamine[15] do appear in the simulation. The sampled MM3*-based maps were

Table 1. ^1H and ^{13}C chemical shifts (*δ*, ppm) and key coupling constants (Hz) for **1** (D_2O, pH 7.0), at 500 MHz and 300 K

	δ^1H (ppm)	*J* (Hz)	$\delta^{13}C$ (ppm)
H1 GlcNAc	4.35	8.7	101
H2 GlcNAc	3.52		70.2
H3 GlcNAc	3.45	10.5	72
H4 GlcNAc	1.75	3.1 (HproR), 5.4 (HproS), 10.2 (H3 GlcNAc), 10.2 (H5 GlcNAc)	40.5
H5 GlcNAc	3.54		76.8
H6 GlcNAc	3.9		62
H6 GlcNAc	3.9		62
HproR	1.56	3.3 (H4 GlcNAc), 10.3 (H1 Gal), 15.5 (HproS)	28.5
HproS	2.01	1.4 (H1 Gal), 5.2 (H4 GlcNAc), 15.5	22.3
H1 Gal	3.22	1.6, 9.9	77.5
H2 Gal	3.3	9.6	71.1
H3 Gal	3.52		73.8
H4 Gal	3.86		69.2
H5 Gal	3.52		78.4
H6 Gal	3.6		70.2
H6 Gal	3.85		70.2
$(CH_2)_7$–CH_3	1.47, 1.2, 0.8		28.5, 25, 31

Table 2. Torsion angle values, relative steric energies and relative population densities of the major conformational low-energy positions of **1** according to MM3* calculations

	Conformer (Φ,Ψ)			
	A (180°/0°)	B (36°/−72°)	C (54°/180°)	D (54°/18°)
ΔE (kJ/mol)	6	7	0	1.5
Population (%)	3	2	85	10

Energy values are given in kJ mol^{-1}.

used to derive the expected $^{3}J_{HH}$ by applying the Haasnoot–Altona modification of the Karplus equation.[16] When the comparison between expected and experimental vicinal proton-proton couplings was performed, the calculated couplings notoriously deviated from the experimental results, highlighted in Tables 1 and 2. In fact, the MM3*-based calculations predict a higher percentage of the unusual *anti*-Ψ conformers around the glycosidic linkage than those actually existing. Moreover, they also predict a higher flexibility around Φ, (averaging of couplings) than that experimentally observed (one large value). The semi-quantitative comparison of expected and experimental *J* values is in agreement with a 60/40 *anti*/*syn* equilibrium around Ψ, with a tentative distribution of 60% C, 20% D, 15% B and 5% A.

According to MM3* calculations (Figs. 1 and 2), compound **1** shows a population density of about 85% around minimum C (*anti*-Ψ). This region is defined by Φ 54° and Ψ 180°. A second region, only destabilized by about 1 kJ/mol, is centered at D (the regular *syn*-*exo*-anomeric orientation), harbors 10% of the population distribution and is defined by Φ 54° and Ψ 18°. Additional minima with relative steric energies above 6 kJ/mol (1.5 kcal/mol) are localized at positions A and B. The respective population densities are 3% for A and 2% for B. A (*anti*-Φ) is defined by Φ,Ψ around 180°/0°, while B is a *syn*-*exo*-anomeric region somehow distorted with Φ/Ψ values of 36/−72°. Therefore, B, C and D adopt the regular *syn*-*exo*-anomeric region around Φ, as for natural *O*-glycosyl compounds. X-ray analysis of *N*-acetyl-lactosamine,[15] has shown that this compound adopts minimum B in the solid state. Therefore, according to the MM3* calculations, *N*-acetyl-lactosamine and its *C*-glycosyl analogue show similar Φ, values, but differ around 180° for Ψ. Moreover, MD simulations revealed that the major minima were conformationally stable during the time scale of the simulations (3 ns).

2.1. NMR Experimental confirmation

The data originating from the MM3* calculations were compared with the experimental results using NMR spectroscopy, mainly *J* and NOE data. Chemical shifts (Table 1) of the individual resonance signals were assigned through a combination of COSY, TOCSY, and HMQC experiments.[16] The presence of the methylene protons in *C*-glycosyl compounds allows the use of coupling constant values to deduce key conformational information around the pseudo-glycosidic torsions. Table 3 shows the expected coupling values (Karplus–Altona[17] equation) for the four local minima of **1** predicted by the MM3* calculations, compared with the experimentally measured values. The experimental coupling values of the *C*-glycosyl analog of *N*-acetyl-lactosamine are indeed similar to those previously described for C-lactose, **7**.[6] Indeed, a similar distribution to that proposed for this compound among minima A–D leads to a satisfactory agreement between expected and observed data.

NOESY Experiments for **1** (Fig. 3) were also performed to assess the conformational distribution. Key NOEs are highlighted in Figure 3, while their corresponding inter-proton distances are presented in Figure 1. It is clear that a short H1′/H3 distance is exclusive to minimum C (*anti*-Ψ), while H1′/H4 interactions represent the existence of population around B and/or D (*syn*-Φ), and H2′/H4 is indicative of the presence of minimum A. Although a quantitative full matrix relaxation approach was performed (Tables 4 and 5) to account for the 'experimental data', visual inspection of the relative H1′/H3 versus H1′/H4 NOE intensities already allowed

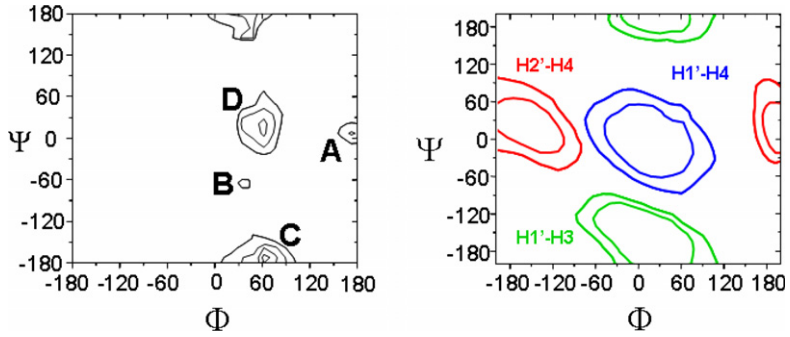

Figure 1. Positions of local minima for **1**, the respective probability distribution, and key interproton distances (between 2.0 and 2.5 Å) for the Φ/Ψ torsion angles. The global minimum, C, is located within the *anti*-Ψ region.

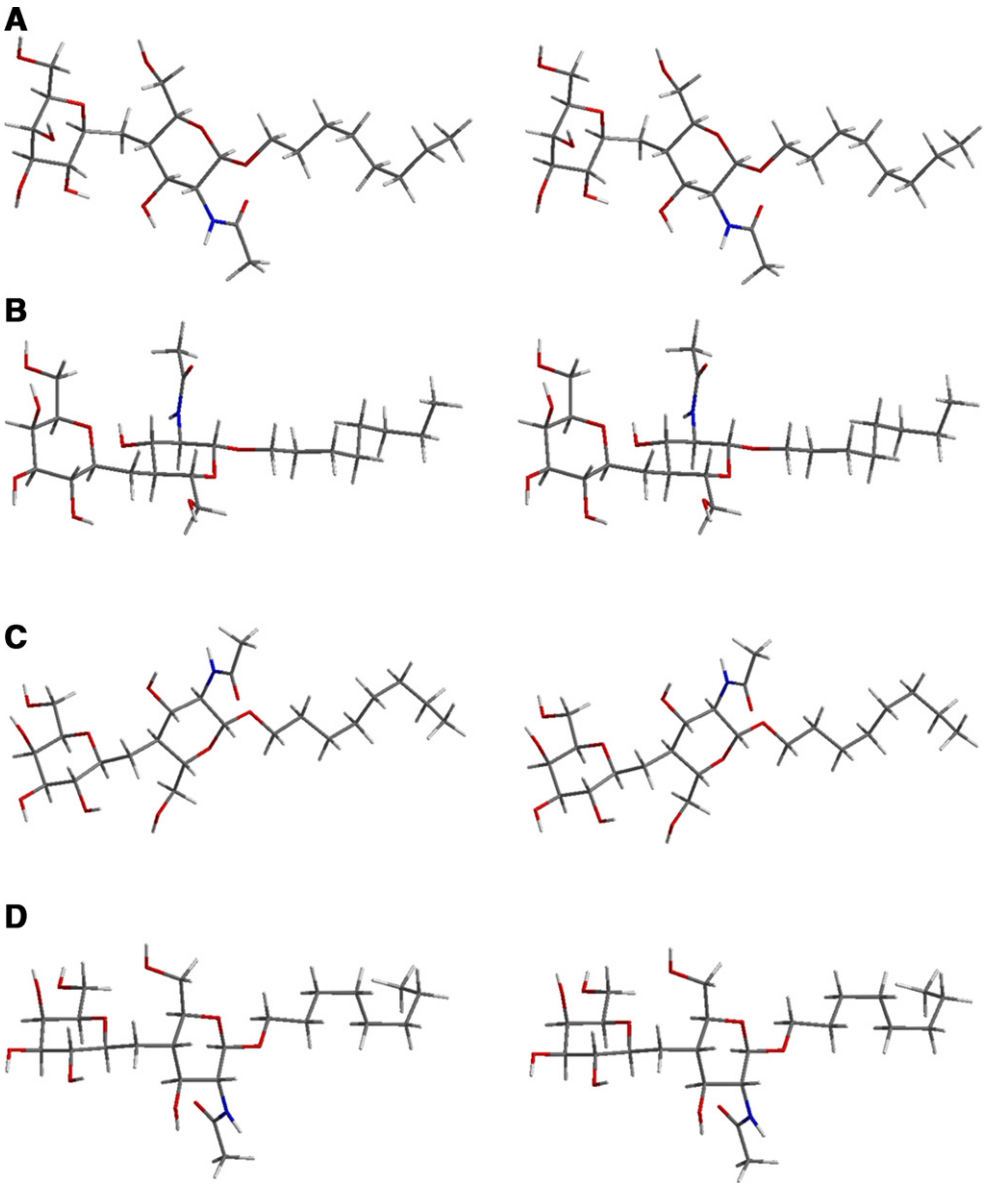

Figure 2. Stereoscopic representation of the different minima, A (180/0), B (36/−72), C (54/18) and D (54/−180), of the *C*-glycosyl analogue of *N*-acetyllactosamine (**1**).

Table 3. *J* Values (Hz) for the local conformational minima and corresponding Φ, Ψ values for **1**

Proton pair	Conformer (*J*, Hz)				Experimental (*J*, Hz)
	A (180°/0°)	B (36°/−72°)	C (54°/−180°)	D (54°/18°)	
$H\text{-}1_{Gal}$/HproS	4.8	1	1.4	1.3	1.4
$H\text{-}1_{Gal}$/HproR	2.3	9.8	11.5	11.3	10.3
$H\text{-}4_{GlcNAc}$/HproS	5	5	3.4	8.4	5.2
$H\text{-}4_{GlcNAc}$/HproR	4.3	11.5	3.7	1.6	3.3

The values were deduced by applying the generalized Karplus equation proposed by Altona to the derived molecular geometries derived from MM3* calculations.

us to demonstrate that the *anti*-Ψ region predominantes in solution compared to the *syn*-Ψ one. The higher value for H1′/H3 (versus H1′/H4) contrasts with the observations for regular *N*-acetyl-lactosamine for which the H1′/H4 NOE is about fourfold more intense than H1′/H3. Moreover, the presence of the H4/H2′ NOE indicates that the region defined by conformer A (*anti*-Φ) is also populated in solution.

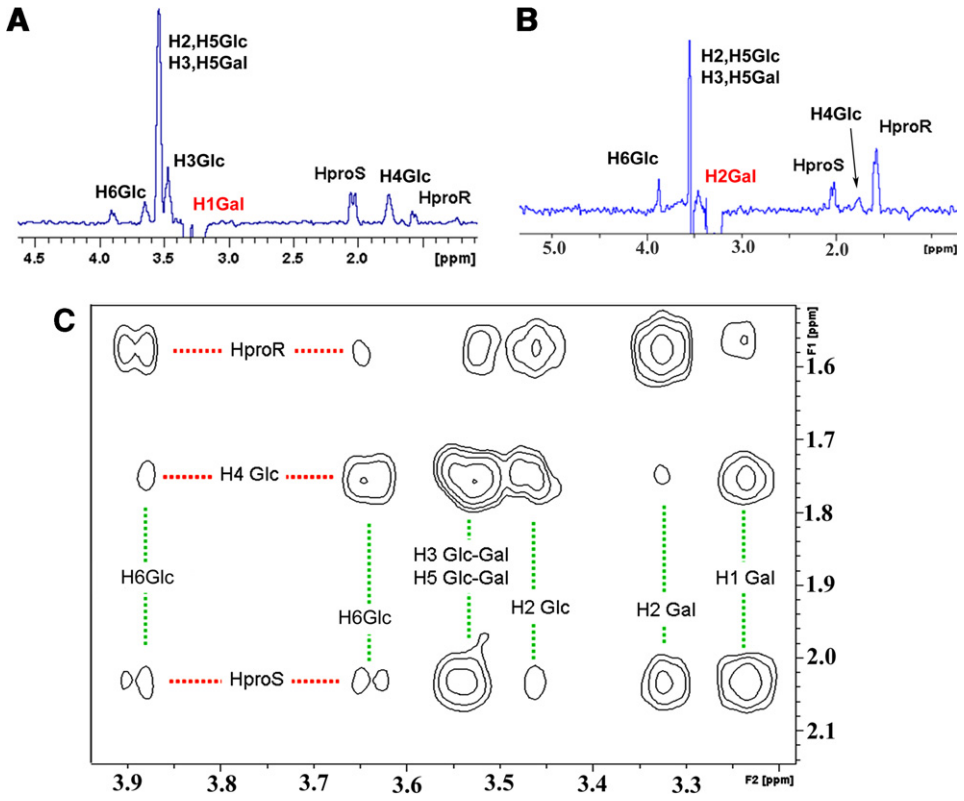

Figure 3. 1D-NOESY spectra (400 ms mixing time) of **1** at 500 MHz and 300 K in D_2O, after selective inversion of H1Gal (A) and H2Gal (B). (C) Enlargement of the key area of the 2D-T-ROESY spectrum (400 ms mixing time) for clarity.

Table 4. Key interproton distances (Å) for the different conformers, the ones corresponding to putative strong NOEs being bolded

	Conformers (Φ/Ψ)			
	A (180°/0°)	B (36°/−72°)	C (54°/−180°)	D (54°/18°)
H1′–H3	4.7	3.5	**2.2**	4.7
H1′–H4	3.7	**2.7**	3.8	**2.6**
H1′–HproR	**2.4**	3.1	3.1	3.1
H1′–H5	4.8	4.7	3.3	4.0
H1′–H6A	4.4	4.6	5.1	**2.4**
H4–H2′	**2.2**	4.7	4.8	4.5
HproS–H4	2.9	**2.3**	**2.4**	3.0
HproS–H5	**2.5**	3.2	4.0	**2.5**
HproS–H6A	3.9	**2.5**	4.0	3.5
HproS–H1′	**2.4**	**2.6**	**2.5**	**2.6**
HproS–H2′	3.8	2.8	3.0	3.0
HproR–H3	**2.4**	2.8	3.9	**2.5**
HproR–H4	2.9	3.1	**2.4**	2.8
HproR–H6A	4.4	3.6	**2.7**	4.4
HproR–H2′	3.2	**2.7**	**2.5**	**2.5**

The protons belonging to the Gal residue are primed.

Table 5. Average distances and calculated NOEs (estimated by applying a full matrix relaxation approach to the ensemble averaged distances computed from the probability distribution map shown in Fig. 1) in comparison with the observed NOEs for compound **1**

Proton pair	%		
	% NOE MM	NOE exp. %	Averaged distance MM (Å)
H1′–H3	8.5	3.6	2.5
H1′–H4	1.5	3.2	3.1
H1′–HproR	4	1.2	2.5
H1′–H5	1.1	0.8	3.3
H1′–H6A	2.1	2.3	2.9
H1′–H6B	<1	1.6	4.6
H4–H2′	<1	0.3	3.8
HproS–H4	3	3.8	2.5
HproS–H5	<1	3	3.3
HproS–H6A	3	—	2.8
HproS–H1′	<1	4.1	3.0
HproS–H2′	4	3	2.5
HproR–H3	3.5	4.6	3.0
HproR–H4	4	4.6	2.5
HproR–H6A	<1	3.1	3.5
HproR–H2′	<1	1.0	3.0

The calculations are shown for a NOE mixing time of 600 ms. The protons belonging to the Gal residue are primed.

Therefore, the MM3*-based population distribution (with C populated up to 85% and D at about 10%) does not reflect the actual conformational equilibrium in water solution, for which four conformers are present in the equilibrium. The comparison of the NOE and *J* values account for a 5% A, 15% B, 60% C, and 20% D. In any case, there is a major contribution of *anti*-Ψ conformers, which is the global minimum of the *C*-glycosyl analogue **1**, which are only marginally populated for the natural β-(1→4) linked oligosaccharides.

Very probably, the increased C–C versus C–O distance at the glycosidic linkage is at the origin of the observed differences between the natural compound and the *C*-glycosyl mimic.[18] Similar differences have been observed in other *C*-glycosyl compounds pointing out that the conformational behavior of *C*-glycosyl compounds cannot be extrapolated to their natural parent compounds, as previously reported.[19]

Moreover, there is a large portion of the energy potential map that is accessible to the glycomimetic, especially in comparison with *N*-acetyl-lactosamine. In principle, the recognition of a given geometry by a receptor must be accompanied by a substantial decrease in conformational entropy,[20] although on the other hand, due to its intrinsic flexibility, compound **1** may be accommodated at different binding sites. Two examples are given below, studying the potent agglutinin/toxin from mistletoe and human galectin-1.

2.2. The bound state. The interaction of 1 with viscumin (mistletoe lectin, VAA) and human galectin-1 (hGal-1)

NMR can be easily used to monitor ligand binding by protein receptors.[21] The most simple manner to assess binding is to analyze line broadening of the ligand signals upon addition of minute amounts of the receptor. Thus, as a first step, respective NMR experiments were performed to monitor binding of **1** to the mistletoe lectin.[22] Figure 4 shows the relevant section of the ^{1}H NMR spectrum of **1** upon addition of VAA, with a **1**/VAA molar ratio of ca. 20:1. Indeed, broadening of the ligand signals is evident, due to the shortening in T_2 relaxation times, promoted by ligand exchange between the free and bound states.[23]

Selective T_1 values are sensitive to the global motion correlation time of a given molecule and, thus, they can also be used to easily monitor ligand binding to large molecular receptors. As shown in Figure 4, the selective T_1 value of H_1-Gal strongly decreases when passing from the free to the bound states, again indicating ligand binding.

Finally, STD experiments[24] were also employed to confirm ligand binding and to try to deduce the binding epitope of the ligand to VAA, which had been assigned in solution primarily to the subdomain 2γ.[22c] Indeed, the largest STD signal intensities were observed for the Gal-residue as deduced from Figure 4. This observation is in agreement with VAA recognizing exclusively the non-

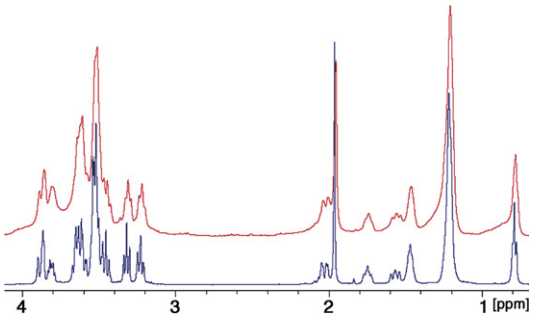

Figure 4a. The 500 MHz ^{1}H NMR spectrum of **1** in the free state (bottom) and in the presence of a 5% molar ratio of VAA (top trace). Ligand–protein ratio is 20:1 and the temperature 298 K. Ligand concentration is 2 mM.

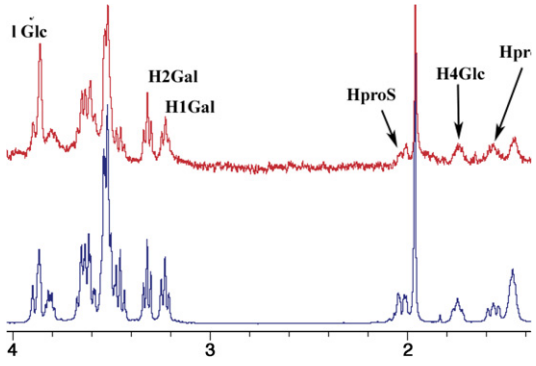

Figure 4b. The 500 MHz STD spectrum after 2 s of on- and off-resonance saturation time (top trace) of **1** in the presence of VAA at a 50:1 ligand–protein molar ratio. Ligand concentration is 2 mM. The major epitope corresponds to the Gal residue. The regular 1D spectrum of **1** is shown below for comparison.

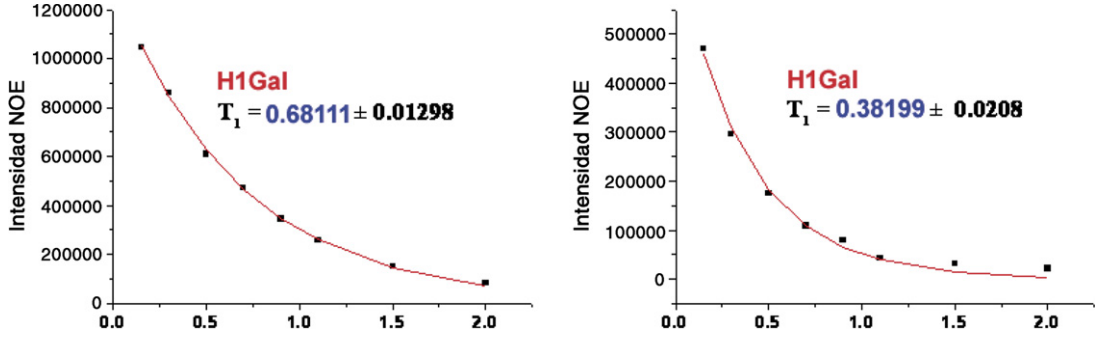

Figure 4c. Representation of the decay of magnetization in an inversion recovery experiments for the estimation of selective T_1 values for H1Gal of **1** in the free state and for a sample containing a 20:1 molar ratio of **1**:VAA. Ligand concentration is 2 mM. The value for the bound state is considerably shortened indicating binding of **1** to VAA.

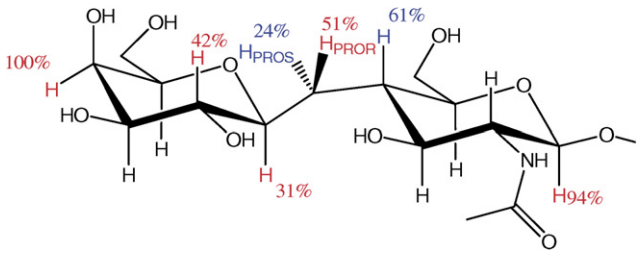

Figure 4d. STD Values measured for **1** in the presence of VAA (50:1 ligand–protein molar ratio). Ligand concentration is 2 mM.

reducing terminal end of Gal-containing oligosaccharides, backed by specificity assays as well as calorimetric and crystallographic evidence.[24] Therefore, **1** behaves as a glycomimetic of *N*-acetyl-lactosamine in its interaction with viscumin.

To examine conformational preferences when both sugar units make contact with the protein, we used human galectin-1 (h-Gal 1) as the receptor. In fact, the presence of the *N*-acetyl group enhances the affinity constant about fourfold.[25] The same protocol described above for the interaction with VAA was applied to deduce binding of **1** to h-Gal 1. Also in this case, line broadening of the resonance signals of **1** and a significant decrease of the selective T_1 value of H1Gal of **1** were observed when a small amount of h-Gal-1 was added to the NMR tube containing **1** (Fig. 5). Both experiments unequivocally indicate ligand binding of **1** to h-Gal-1.

Finally, trNOESY experiments were performed to address the issue to define the bound conformation of **1** to h-Gal 1. As previously shown for ligands that are not bound tightly and exchange between free and bound

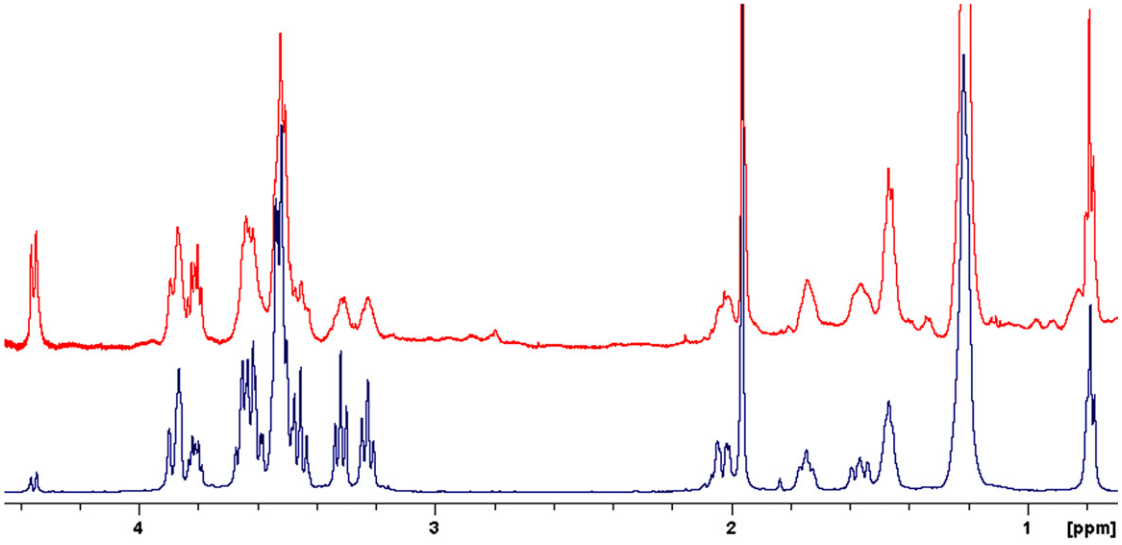

Figure 5a. The ^{1}H NMR spectrum of **1** in the free state (bottom) and in the presence of a 5% molar ratio of h-Gal 1 (top trace). Ligand–protein ratio is 20:1. Ligand concentration is 2 mM.

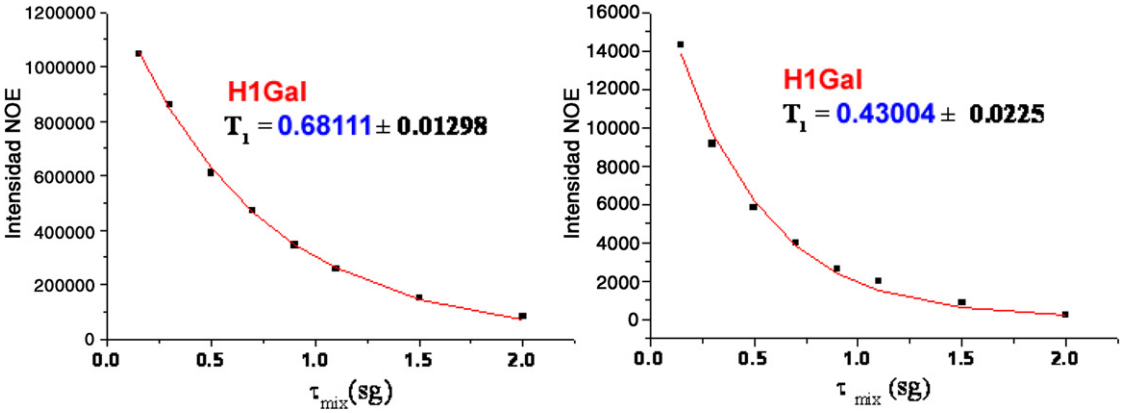

Figure 5b. Representation of the decay of magnetization in an inversion recovery experiments for the estimation of selective T_1 values for H1Gal of **1** in the free state and for a sample containing a 20:1 molar ratio of **1**:h-Gal-1. Ligand concentration is 2 mM. The value for the bound state is considerably shortened indicating binding of **1** to h-Gal-1.

state at a reasonably fast rate, the transferred nuclear Overhauser enhancement experiment provides an adequate mean to determine the conformation of the bound ligand.[26]

trNOESY data were collected using a variety of mixing times and two ligand/protein molar ratios, namely 12:1 and 25:1. In all cases, negative cross-peaks were clearly observed at 300 K, as expected for ligand binding (Fig. 6), in contrast to observations for the free ligand, for which positive NOEs were observed.[27]

Figure 6 shows the NOESY spectra of **1**, when free in solution and bound to h-Gal 1 (trNOESY). As described above, there are four conformational families in equilibrium for the free molecule in solution, with two major ones, dubbed C and D, which only differ in the orientation around Ψ angle. The exclusive NOEs for these regions are H1Gal/H3GlcNAc and H1Gal/H4GlcNAc, respectively. The trNOESY data were analyzed by employing the CORCEMA approach,[28] which uses a full relaxation matrix approach in the presence of exchange. The experimental proton–proton distances in the bound state indicate that both six-membered rings are not distorted after interaction with the lectin binding site, as deduced from the experimental H1/H3 and/or H1/H5 distances for both the Gal and GlcNAc residues. The H2Gal/H4GlcNAc inter-proton distance is rather long, as deduced from the corresponding weak intensity. Thus, h-Gal-1 does not accommodate the *anti*-Φ conformation. The experimentally determined H1Gal/H3GlcNAc distance in the bound state is above 3 Å. Therefore, the major conformation in the free state, *anti*-Ψ, is not present when bound to this lectin revealing the presence of a conformational selection process. The H1Gal/H4GlcNAc distance, which supports the presence of the *exo*-Φ/*syn*-Ψ conformer present in about 35% of the population in the free state is around 2.5 Å, indicating the preferential selection of this local minimum by h-gal-1 for binding. Moreover, the intense H6GlcNAc/HproS NOE indicates that the molecule adopts a *syn*-Φ orientation when in the lectin site. Thus, all these experimental data indeed indicate that the *exo*-Φ/*syn*-Ψ conformer is the major geometry adopted by the *C*-glycosyl analogue of *N*-acetyl *C*-lactosamine when in contact with h-Gal 1.

In conclusion, only one of the four existing conformers in solution for **1** is indeed bound by h-Gal-1. Because this conformer is only populated to an extent of 35% in the free state, its geometry harbors favorable characteristic for the conformational selection process. These results support, in a definitive manner, the exclusive recognition of *syn*-type conformations around both *Φ*/*Ψ* torsión angles of β-linked galactosides by galectins.[15] In fact, in the X-ray structure of different lactose derivatives bound to galectins,[15] besides the typical key interactions between the nonreducing end galactoside residue (hydrogen bonds and aromatic-sugar interactions), there is a key hydrogen bond between the OH-3 group of the Glc(GlcNAc) and a properly oriented polar lateral chain of the polypeptide moiety.[27] This key hydrogen bond is only possible if the natural disaccharide (or glycomimetics thereof) adopts a *syn*-type

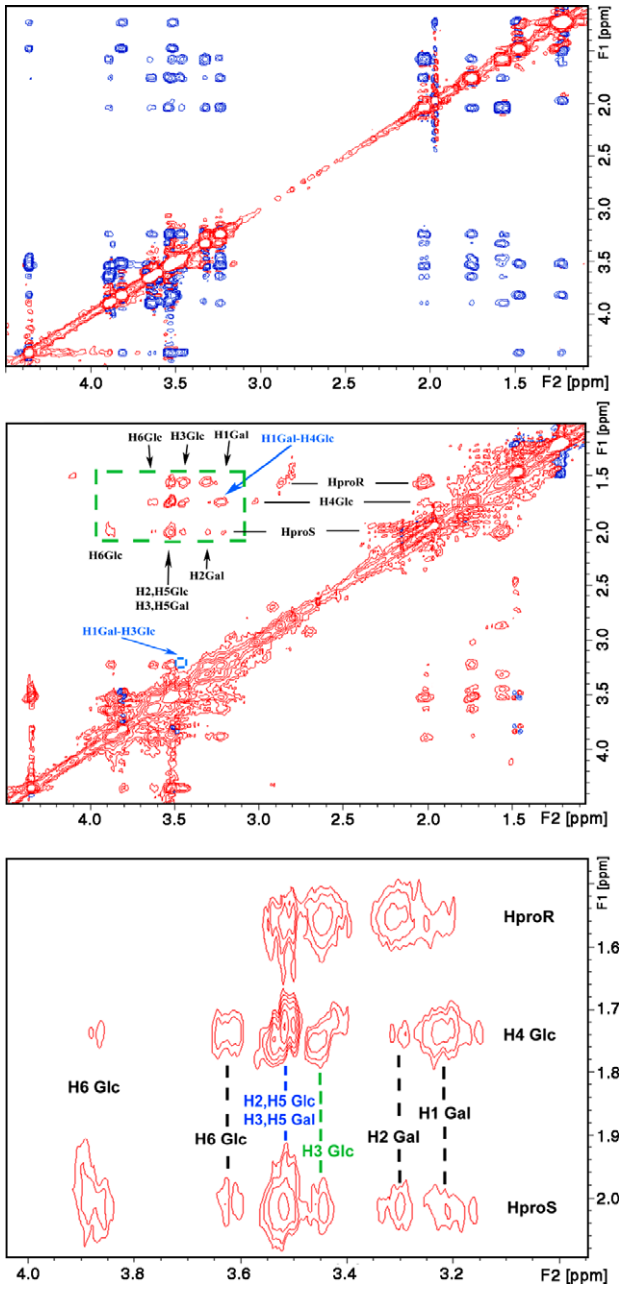

Figure 6. Top: NOESY spectrum (mixing time 700 ms) for free **1** in D_2O solution. Cross peaks have different sign to diagonal peaks. Middle: TRNOESY spectrum (mixing time 200 ms) for a 20:1 molar ratio of **1**: hGal-1 (0.1 mM of lectin). Cross-peaks have the same sign as diagonal peaks. No H1Gal–H3GlcNAc contact is observed, indicating that the *anti*-Ψ conformer is not bound by this lectin. Bottom: Expansion of the key region of the TRNOESY spectrum. Preferential recognition of the *syn*-Ψ conformer is evident due to the presence of a strong H1Gal-H4 GlcNAc cross-peak.

around Φ/Ψ. Therefore, it is likely that this hydrogen bond could be the key driving force for the conformational selection process that permits the recognition of the minor conformer in free solution, also observed for galactosyl xylopyranosides.[30]

3. Materials and methods

3.1. Molecular mechanics and dynamics calculations

The conformation of **1** in the free state was analyzed by standard NMR methods and molecular mechanics calculations. The initial calculations were performed on both the C- and O-disaccharide analogues (**1ab)** using the MM3* force field[13] as implemented in MACROMODEL 4.5.[12] Potential energy maps were calculated as described,[29] because this is a β-(1→4)-linked disaccharide, similar to C-lactose, which has been extensively studied.[6] Φ is defined as H-1′–C-1′–O–C4 and Ψ as C1′–O–C4–H4. Additionally, MD calculations were also performed with the same force field. In particular, three independent unrestrained MD simulations for a total period of 5 ns were run starting from the different local minima.

3.2. NMR Spectroscopy

The NMR experiments were performed at 500 MHz on Bruker AVANCE spectrometers, using temperatures between 298 and 318 K and concentrations between 1 and 2 mM. A 1D ^{1}H NMR spectrum of **1** was also recorded at 800 MHz to access the vicinal coupling constant values. The best *J* values were estimated by computer simulation of the 1D spectrum with the Mestre *J* software.

For the experiments with the free ligands, the corresponding compound was dissolved in D_2O, and the solution was degassed by passing argon through the solution. COSY, TOCSY (80 ms, mixing time), and ge-HSQC experiments were performed using standard. 2D T-ROESY experiments were carried out with mixing times of 300, 400, and 500 ms.[30] The strength of the 180° pulses during the spin lock period were attenuated four times with respect to that of the 90° hard pulses (between 7.2 and 7.5 μs). To deduce the interproton distances, relaxation matrix calculations were performed using software written at home, that is available from the authors upon request.

Mistletoe agglutinin and human galectin-1 were purified and subjected to rigorous activity and quality controls as described.[22,30,31] STD and trNOE experiments were performed at 500 MHz. First, each lectin was subjected to two cycles of freeze–drying with D_2O to remove traces of H_2O and then transferred in phosphate buffer solution (pH 5.5) solution into the NMR tube at a final concentration of ca. 0.05 (STD), 0.1, and 0.2 mM (trNOESY). trNOESY experiments were performed with mixing times of 150, 200, and 250 ms, for molar ratios between 15:1 and 50:1 of **1**:lectin. No purging spin-lock period to remove the background of protein signals was employed. In all cases, line broadening of the sugar protons was monitored after the addition of the ligand. STD experiments were carried out by using the method proposed by Meyer and co-workers.[23] A blank experiment was also performed by applying on- and off-resonance saturation on a sample containing only the free ligand. No STD was observed under these conditions. In all cases, no saturation of the residual HDO signal was performed and, again, no spin-lock pulse was employed. In our hands, the use of a spin-lock period induced artifacts in the difference spectrum.

The theoretical analysis of the trNOEs of the sugar protons was performed using a relaxation matrix with exchange, using the CORCEMA program,[28] as described.[16] Different exchange-rate constants were used to obtain the optimal match between experimental and theoretical results of the intraresidue H-1/H-3 and H-1/H-3 cross-peaks of GlcNAc and Gal moieties for a given protein/ligand ratio. Normalized intensity values were used because they allow correction for spin-relaxation effects. The overall correlation time τ_c for the free state was always set to 0.23 ns and the τ_c for the bound state for galectin-1 and mistletoe were estimated as 20 and 35 ns, respectively. To fit the experimental trNOE intensities, different exchange-rate constants were tested. The best fit was obtained by employing a K_d of 5×10^{-4} M and off-rate constants of ca. 300 s^{-1}.[29] trROESY experiments were also carried out to exclude spin-diffusion effects. A continuous wave spin lock pulse was used during the 150 ms mixing time. Key NOEs were shown to be direct cross-peaks, because they exhibited different sign to diagonal peaks.

Acknowledgement

Financial support by the Ministry of Education and Science of Spain is gratefully acknowledged (CTQ-2006-10874-C02-01), as is a EC Marie Curie Research Training Network Grant (Contract No. MRTN-CT-2005-019561). The CAI-NMR facility at the University Complutense of Madrid is thanked for the access to the 500 MHz spectrometer. We also appreciate the support of Professor. N. R. Krishna (University of Birmingham, AL, USA) for the use of CORCEMA program for trNOESY analysis.

References

1. (a) Levy, D. E.; Tang, C. *The Chemistry of C-Glycosides*; Elsevier Science: Oxford, 1995; (b) Skrydstrup, T.; Vauzeilles, B.; Beau, J.-M. Synthesis of *C*-Oligosaccharides. In *Carbohydrates in Chemistry and Biology*; Ernst, B., Hart,

G. W., Sinay, P., Eds.; Wiley-VCH: Weinheim, 2000; Vol. 1, pp 495–530; (c) Liu, L.; McKee, M.; Postema, M. H. D. *Curr. Org. Chem.* **2001**, *5*, 1133–1167; (d) Beau, J.-M.; Vauzeilles, B.; Skrydstrup, T. *C*-Glycosyl Analogs of Oligosaccharides and Glycosyl Amino Acids. In *Glycoscience*; Fraser-Reid, B. O., Tatsuta, K., Thiem, J., Eds.; Springer: Berlin, 2001; Vol. 3, pp 2679–2724.
2. (a) Wang, Y.; Goekjian, P. G.; Ryckman, D. M.; Miller, W. H.; Babirad, S. A.; Kishi, Y. *J. Org. Chem.* **1992**, *57*, 482–489; (b) Kishi, Y. *Pure Appl. Chem.* **1993**, *65*, 771–778; (c) Goekjian, P. G.; Wei, A.; Kishi, Y. Conformational Analysis of C-glycosides and Related Compounds: Programming Conformational Profiles of C- and O-Glycosides. In *Carbohydrate-Based Drug Discovery*; Wong, C.-H., Ed.; Wiley-VCH: Weinheim, 2003; Vol. 1, pp 305–340.
3. Jiménez-Barbero, J.; Espinosa, J. F.; Asensio, J. L.; Cañada, F. J.; Poveda, A. The Conformation of *C*-Glycosyl Compounds. In *Adv. Carbohydr. Chem. Biochem.*; Horton, D., Ed.; Academic Press, 2001; Vol. 56, pp 235–284.
4. Espinosa, J. F.; Bruix, M.; Jarreton, O.; Skrydstrup, T.; Beau, J.-M.; Jiménez-Barbero, J. *Chem. Eur. J.* **1999**, *5*, 442–448.
5. (a) Sinaÿ, P. *Pure & Appl. Chem.* **1997**, *69*, 459–463; (b) Colliou, V. Ph.D. Thesis, Université Pierre et Marie Curie Paris 6, 1997.
6. (a) Asensio, J. L.; Jimenez-Barbero, J. *Biopolymers* **1995**, *35*, 55–73; (b) Espinosa, J. F.; Martín-Pastor, M.; Asensio, J. L.; Dietrich, H.; Martín-Lomas, M.; Schmidt, R. R.; Jiménez-Barbero, J. *Tetrahedron Lett.* **1995**, *36*, 6329–6332.
7. (a) Asensio, J. L.; Cañada, F. J.; Jiménez-Barbero, J. *Eur. J. Biochem.* **1995**, *233*, 618–630; (b) Espinosa, J.-F.; Cañada, F. J.; Asensio, J. L.; Martín-Pastor, M.; Dietrich, H.; Martín-Lomas, M.; Schmidt, R. R.; Jiménez-Barbero, J. *J. Am. Chem. Soc.* **1996**, *118*, 10862–10871; (c) Asensio, J. L.; Espinosa, J. F.; Dietrich, H.; Cañada, F. J.; Schmidt, R. R.; Martín-Lomas, M.; André, S.; Gabius, H.-J.; Jiménez-Barbero, J. *J. Am. Chem. Soc.* **1999**, *121*, 8995–9000; (d) Gabius, H.-J.; Siebert, H.-C.; André, S.; Jiménez-Barbero, J.; Rüdiger, H. *ChemBioChem* **2004**, *5*, 740–764.
8. (a) Reuter, G.; Gabius, H.-J. *Cell. Mol. Life Sci.* **1999**, *55*, 368–422; (b) Rüdiger, H.; Siebert, H.-C.; Solís, D.; Jiménez-Barbero, J.; Romero, A.; von der Lieth, C.-W.; Díaz-Mauriño, T.; Gabius, H.-J. *Curr. Med. Chem.* **2000**, *7*, 389–418; (c) Gabius, H.-J. *Crit. Rev. Immunol.* **2006**, *26*, 43–79; (d) Wu, A. M.; Singh, T.; Wu, J. H.; Lensch, M.; André, S.; Gabius, H.-J. *Glycobiology* **2006**, *16*, 524–537.
9. (a) Gabius, H.-J. *Biochimie* **2001**, *83*, 659–666; (b) André, S.; Kaltner, H.; Furuike, T.; Nishimura, S.-I.; Gabius, H.-J. *Bioconjugate Chem.* **2004**, *15*, 87–98; (c) Jiménez, M.; Sáiz, J. L.; André, S.; Gabius, H.-J.; Solıs, D. *Glycobiology* **2005**, *15*, 1386–1395; (d) Smetana, K., Jr.; Dvořánková, B.; Covance, M.; Bouček, J.; Klíma, J.; Motlík, J.; Lensch, M.; Kaltner, H.; André, S.; Gabius, H.-J. *Histochem. Cell Biol.* **2006**, *125*, 171–182; (e) Villalobo, A.; Nogales-González, A.; Gabius, H.-J. *Trends Glycosci. Glycotechnol.* **2006**, *18*, 1–37.
10. Carpintero, M.; Bastida, A.; Garcia-Junceda, E.; Jimenez-Barbero, J.; Fernandez-Mayoralas, A. *Eur. J. Org. Chem.* **2001**, 4127–4135.
11. For the application of molecular mechanics force fields to the conformational analysis of carbohydrate molecules, see: Perez, S.; Imberty, A.; Engelsen, S.; Gruza, J.; Mazeau, K.; Jimenez-Barbero, J.; Poveda, A.; Espinosa, J. F.; van Eyck, B. P.; Johnson, G.; French, A. D.; Kouwijzer, M. L. C. E.; Grootenuis, P. D. J.; Bernardi, A.; Raimondi, L.; Senderowitz, H.; Durier, V.; Vergoten, G.; Rasmussen, K. *Carbohydr. Res.* **1998**, *314*, 141–155.
12. See, for instance, *Computer Modelling of Carbohydrate Molecules*; French, A. D., Brady, J. W., Eds.; American Chemical Society: Washington, DC, 1990.
13. Allinger, N. L.; Yuh, Y. H.; Lii, J. H. *J. Am. Chem. Soc.* **1989**, *111*, 8551–8566.
14. Mohamadi, F.; Richards, N. G. J.; Guida, W. C.; Liskamp, R.; Lipton, M.; Caufield, C.; Chang, G.; Hendrickson, T.; Still, W. C. *J. Comp. Chem.* **1990**, *11*, 440–467.
15. Longchambon, F.; Ohanessian, J.; Gillier-Pandrand, H.; Duchet, D.; Jacquinet, J. C.; Sinaÿ, P. *Acta Crystallogr. B* **1971**, *37*, 601–607.
16. For a survey of NMR methods applied to saccharide molecules, see: *NMR Spectroscopy of Glycoconjugates*; Jiménez-Barbero, J., Peters, T., Eds.; Wiley-VCH: Weinheim, 2002.
17. Haasnoot, C. A. G.; de Leeuw, F. A. A. M.; Altona, C. *Tetrahedron* **1980**, *36*, 2783–2792.
18. Martin-Pastor, M.; Espinosa, J. F.; Asensio, J. L.; Jimenez-Barbero, J. *Carbohydr. Res.* **1997**, *298*, 15–49.
19. For instance, see accompanying papers in this issue: Vidal, P.; Vauzeilles, B.; Blériot, Y.; Sollogoub, M.; Sinaÿ, P.; Espinosa, J. F.; Jiménez-Barbero, J. *Carbohydr. Res.*, submitted for publication.
20. Hunter, C. A. *Angew Chem., Int. Ed.* **2004**, *43*, 5310–5324.
21. See, for instance: Jahnke, W.; Florsheimer, A.; Blommers, M. J. J.; Paris, C. G.; Nalin, C. M.; Pérez, L. B. *Curr. Topics Med. Chem.* **2003**, *3*, 69–80.
22. (a) Gabius, H.-J. *Anal. Biochem.* **1990**, *189*, 91–94; (b) Gabius, H.-J.; Darro, F.; Remmelink, M.; André, S.; Kopitz, J.; Danguy, A.; Gabius, S.; Salmon, I.; Kiss, R. *Cancer Invest.* **2001**, *19*, 114–126; (c) Jiménez, M.; André, S.; Siebert, H.-C.; Gabius, H.-J.; Solís, D. *Glycobiology* **2006**, *16*, 926–937.
23. Mayer, M.; Meyer, B. *J. Am. Chem. Soc.* **2001**, *123*, 6108–6117.
24. (a) Galanina, O. E.; Kaltner, H.; Khraltsova, L. S.; Bovin, N. V.; Gabius, H.-J. *J. Mol. Recognit.* **1997**, *10*, 139–147; (b) Bharadwaj, S.; Kaltner, H.; Korchagina, E. Y.; Bovin, N. V.; Gabius, H.-J.; Surolia, A. *Biochim. Biophys. Acta* **1999**, *1472*, 191–196; (c) Niwa, H.; Tonevitsky, A. G.; Agapov, I. I.; Saward, S.; Pfüller, U.; Palmer, R. A. *Eur. J. Biochem.* **2003**, *270*, 2739–2749.
25. Ahmad, N.; Gabius, H.-J.; Kaltner, H.; André, S.; Kuwabara, I.; Liu, F.-T.; Oscarson, S.; Norberg, T.; Brewer, C. F. *Can. J. Chem.* **2002**, *80*, 1096–1104.
26. See, for instance: (a) Bevilacqua, V. L.; Thomson, D. S.; Prestegard, J. H. *Biochemistry* **1990**, *29*, 5529–5537; (b) Bevilacqua, V. L.; Kim, Y.; Prestegard, J. H. *Biochemistry* **1992**, *31*, 9339–9349.
27. Neuhaus, D.; Williamson, M. P. The Nuclear Overhauser Effect. In *Structural and Conformational Analysis*; VCH: New York, 1989.
28. (a) Moseley, H. N. B.; Curto, E. V.; Krishna, N. R. *J. Magn. Reson., Ser. B* **1995**, *108*, 243–261; (b) Krishna, N. R.; Moseley, H. N. B. *Biol. Magn. Reson.* **1999**, *17*, 223–307.
29. López-Lucendo, M. F.; Solis, D.; Andre, S.; Hirabayashi, J.; Kasai, K.; Kaltner, H.; Gabius, H. J.; Romero, A. *J. Mol. Biol.* **2004**, *343*, 957–970.
30. Alonso-Plaza, J. M.; Canales, M. A.; Jimenez, M.; Roldan, J. L.; Garcia-Herrero, A.; Iturrino, L.; Asensio, J. L.; Canada, F. J.; Romero, A.; Siebert, H. C.; André, S.;

Solís, D.; Gabius, H.-J.; Jiménez-Barbero, J. *Biochim. Biophys. Acta* **2001**, *1568*, 225–236.
31. (a) Siebert, H.-C.; André, S.; Lü, S.-Y.; Frank, M.; Kaltner, H.; van Kuik, J. A.; Korchagina, E. Y.; Bovin, N. V.; Tajkhorshid, E.; Kaptein, P.; Vliegenthart, J. F. G.; von der Lieth, C.-W.; Jiménez-Barbero, J.; Kopitz, J.; Gabius, H.-J. *Biochemistry* **2003**, *42*, 14762–14773; (b) André, S.; Kojima, S.; Prahl, M.; Lensch, M.; Unverzagt, C.; Gabius, H.-J. *FEBS J.* **2005**, *272*, 1986–1998.